THz-Frequency Modulation of the Hubbard U in an Organic Mott Insulator

R. Singla,[1,*] G. Cotugno,[1,2] S. Kaiser,[1,7,8,†] M. Först,[1] M. Mitrano,[1] H. Y. Liu,[1] A. Cartella,[1] C. Manzoni,[1,4] H. Okamoto,[5] T. Hasegawa,[6] S. R. Clark,[2,9] D. Jaksch,[2,3] and A. Cavalleri[1,2,‡]

[1]*Max Planck Institute for the Structure and Dynamics of Matter, Luruper Chaussee 149, 22761 Hamburg, Germany*
[2]*Department of Physics, Oxford University, Clarendon Laboratory, Parks Road, OX1 3PU Oxford, United Kingdom*
[3]*Centre for Quantum Technologies, National University of Singapore, 3 Science Drive 2, Singapore 117543, Singapore*
[4]*IFN-CNR, Dipartimento di Fisica-Politecnico di Milano, Milan, Italy*
[5]*Department of Advanced Material Science, University of Tokyo, Chiba 277-8561, Japan*
[6]*National Institute of Advanced Industrial Science and Technology (AIST), Tsukuba 305-8562, Japan*
[7]*Max Planck Institute for Solid State Research, Heisenbergstraße 1, 70569 Stuttgart, Germany*
[8]*4th Physics Institute, University of Stuttgart, Pfaffenwaldring 57, 70550 Stuttgart, Germany*
[9]*Department of Physics, University of Bath, Claverton Down, Bath BA2 7AY, United Kingdom*

(Received 3 September 2014; revised manuscript received 24 July 2015; published 29 October 2015)

We use midinfrared pulses with stable carrier-envelope phase offset to drive molecular vibrations in the charge transfer salt ET-F_2TCNQ, a prototypical one-dimensional Mott insulator. We find that the Mott gap, which is probed resonantly with 10 fs laser pulses, oscillates with the pump field. This observation reveals that molecular excitations can coherently perturb the electronic on-site interactions (Hubbard U) by changing the local orbital wave function. The gap oscillates at twice the frequency of the vibrational mode, indicating that the molecular distortions couple quadratically to the local charge density.

DOI: 10.1103/PhysRevLett.115.187401 PACS numbers: 78.30.-j, 71.30.+h, 78.40.Me, 78.47.jh

Nonlinear phononics, the coherent excitation of anharmonically coupled collective lattice modes, can be used to create transient crystal structures with new electronic properties [1]. Examples of such nonlinear phonon control are ultrafast insulator-metal transitions [2], melting of magnetism [3], and light-induced superconductivity [4–6]. Nonlinear phononics has been realized and understood in the limit of cubic anharmonic coupling [7,8], which results in rectification of an excited lattice oscillation and in the net displacement of the atomic positions along a second vibrational mode. Change in the electronic properties results then from the altered bond angles and nearest-neighbor atomic distances [9], which perturb hopping amplitudes and exchange interactions. However, local parameters like Mott correlations, of importance in many complex materials, are not modulated by nonlinear phononics.

In this Letter, we show that the on-site Coulomb integral can be modulated in molecular solids by driving local molecular degrees of freedom to large amplitudes [10,11]. The excitation of local modes at midinfrared frequencies is different from the case of nonlinear phononics in that the molecular orbital and, concomitantly, the on-site charge density are controlled [12,13], with each site maintained in its electronic ground state.

A Mott insulator is a half-filled solid in which electrons are made immobile by their mutual Coulomb repulsion. This physics is often described by the extended Hubbard Hamiltonian

$$\hat{H} = -t\sum_{j\sigma}(\hat{c}^{+}_{j\sigma}\hat{c}_{j+1\sigma} + \text{H.c.}) + V\sum_{j}\hat{n}_j\hat{n}_{j+1} + U\sum_{j}\hat{n}_{j\uparrow}\hat{n}_{j\downarrow}, \quad (1)$$

where U and V represent on-site and nearest-neighbor-site Coulomb repulsions, and t denotes the tight-binding hopping amplitude [14,15]. In Eq. (1), $\hat{c}^{\dagger}_{j\sigma}$ ($\hat{c}_{j\sigma}$) is the creation (annihilation) operator for an electron at site j with spin σ, while $\hat{n}_{j\sigma}$ is the associated number operator and $\hat{n}_j = \hat{n}_{j\uparrow} + \hat{n}_{j\downarrow}$. The key features of the Hubbard model are well reproduced in some molecular solids and, in one dimension, by the charge transfer salt Bis-(ethylendithyo)-tetrathiafulvalene-difluorotetracyano-quinodimethane (ET-F_2TCNQ). The crystal structure of this material is shown in Fig. 1(a). One-dimensional Mott physics is observed along the crystallographic a axis, where a half-filled chain of ET molecules is characterized by small intersite tunneling amplitude ($t \sim 40$ meV) and large Coulomb repulsion ($V \sim 120$ meV and $U \sim 840$ meV). Hence, although the system is fractionally filled, a large correlation gap is found. As shown in Fig. 1(b), the reflectivity spectrum of ET-F_2TCNQ exhibits a sharp charge transfer band centered at 5500 cm^{-1} [16]. Note the small electron-lattice interaction in ET-F_2TCNQ [17] is insufficient to drive a Peierls distortion, so that Mott physics is retained down to very low temperatures. Moreover, since our experiments are performed at room temperature, far above the 30 K Néel temperature [16] and $U \gg k_B T \gg t^2/U$, no long-range Néel spin order is present.

In this and other charge transfer crystals, one finds collective phonon modes only at very low frequencies, well separated from higher-frequency localized molecular vibrations, which are observed in the midinfrared. Here we consider the physical situation discussed schematically in Fig. 2. A single localized vibration of the ET molecule

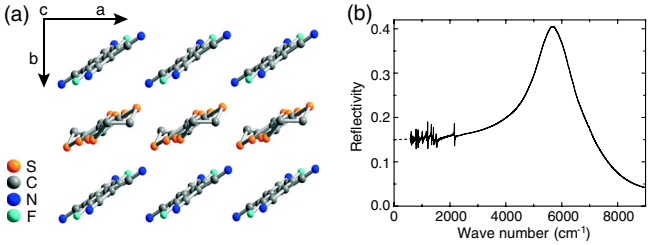

FIG. 1 (color online). (a) The crystal structure of one-dimensional organic salt ET-F_2TCNQ (yellow, ET; blue, F_2TCNQ). (b) Static reflectivity of the compound with electric field parallel to crystallographic a axis (along the ET chain).

is resonantly driven along the electric field of a midinfrared optical pulse. This vibrational excitation leads to a time-dependent deformation of the valence orbital wave function and variation of local charge densities at twice the frequency of the driving field. This, in turn, modulates the Hamiltonian parameters introduced in Eq. (1). To account for this physics, extra terms are added whose form is justified as follows: First, we assume that the classical vibrational mode coordinate q_j only couples to the local charge density and neglect the coupling to other lattice modes [18]. In general, this gives additional terms of the form $\hat{n}_j f(q_j) + \hat{n}_{j\uparrow}\hat{n}_{j\downarrow} g(q_j)$, where $f(q_j)$ and $g(q_j)$ are two functions of the local mode coordinate that are not known *a priori*. Expanding the functions f and g as a series, we obtain

$$\hat{H}_{e\text{-vib}} = \sum_j \hat{n}_j (A_1 q_j + A_2 q_j^2 + \cdots) + \sum_j \hat{n}_{j\uparrow}\hat{n}_{j\downarrow}(B_1 q_j + B_2 q_j^2 + \cdots). \quad (2)$$

Since the molecule is centrosymmetric and the vibrational mode is of odd symmetry, the terms linear in q_j [19,20], which dominate the coupling for all even modes, vanish ($A_1 = B_1 = 0$). As the vibrational mode's natural frequency is Ω_{IR}, every molecule is coherently driven by the laser pulse with its coordinate in time τ described as $q_j(\tau) = q_{\mathrm{IR}}(\tau) = C\sin(\Omega_{\mathrm{IR}}\tau)$, where C is the driving amplitude. This implies that the A_2 term $\propto q_{\mathrm{IR}}^2(\tau)\sum_j \hat{n}_j$ couples to the total density, resulting in an irrelevant global phase shift. We are, therefore, left with a quadratic coupling to the on-site interaction of the form $\hat{H}_{e\text{-vib}} = B_2 q_{\mathrm{IR}}^2(\tau)\hat{n}_{j\uparrow}\hat{n}_{j\downarrow} = (C/2)B_2[1-\cos(2\Omega_{\mathrm{IR}}\tau)]\hat{n}_{j\uparrow}\hat{n}_{j\downarrow}$. Importantly, the coefficient $B_2 < 0$ because the vibration will, in general, cause the valence orbital to spatially expand.

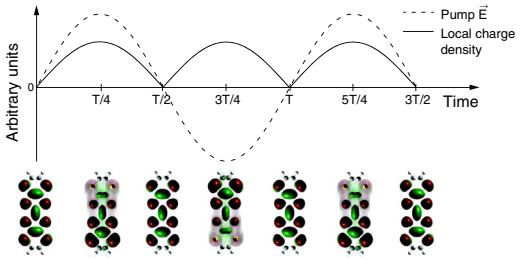

FIG. 2 (color online). (a) Temporal evolution of the pump electric field (dashed black line) together with the resultant change in the local charge density (solid black line) and the corresponding orbital motion of vibrationally excited ET molecule over time.

Thus, two effects are expected as long as an odd molecular mode is driven: a time-averaged reduction of the on-site repulsion together with its modulation at $2\Omega_{\mathrm{IR}}$.

These predictions can be tested only by exciting vibrational oscillations by midinfrared pump pulses with a stable carrier-envelope phase (CEP), in which the temporal offset between the electric field and the intensity envelope is constant and locked over consecutive laser shots. Hence, every laser pulse drives the molecule with identical phase and allows measurements performed with subcycle resolution over many pump pulses. The evolution of these oscillations is then monitored by a delayed probe pulse. The time resolution of this experiment is given by the probe-pulse duration, which should be of the order of one-half of the vibrational period to resolve effects at Ω_{IR} and one-quarter to observe oscillations at $2\Omega_{\mathrm{IR}}$. In the experiments on ET-F_2TCNQ discussed here, a 10 μm vibrational mode with a period of 33 fs is excited, requiring probe pulses of approximately 8 fs duration, tuned to the 700 meV charge transfer resonance. Note that this pulse duration corresponds to less than two optical cycles at the corresponding probe wavelength of 1.7 μm.

In order to generate the required ultrashort probe pulses, the following system was developed. Midinfrared optical pulses with locked carrier-envelope phase were obtained by difference frequency generation from two near-infrared (NIR) optical parametric amplifiers (OPAs) driven by an amplifed Ti:sapphire laser operating at 800 nm wavelength and at 1 kHz repetition rate. The two OPAs were seeded by replicas of a single white-light continuum to preserve their relative phase; difference frequency mixing between the two NIR-amplified sources occurring in a GaSe crystal generated passively CEP-stable 130 fs pulses tunable in the midinfrared region [21]. To compensate for slow thermal drifts, these pulses were actively stabilized in phase [22] and used to drive the infrared-active molecular mode of ET-F_2TCNQ at 10 μm wavelength (30 THz frequency), perpendicular to the a axis [see Fig. 3(a)]. The system was probed by 700 meV pulses derived from a third near-infrared OPA pumped by another portion of the 800 nm Ti:sapphire laser source. The broadband probe pulses, an order of magnitude weaker than the pump pulse, covered the spectral region between 570 and 980 meV (4600–7900 cm^{-1}) as shown in Fig. 3(a); their duration was compressed to approximately 10 fs, close to the transform limit, using a deformable mirror in a grating-based 4-f pulse shaper [23]. Figure 3(b) shows the measured phase-locked electric field of the pump pulse and the intensity envelope of the probe pulse. The probe beam was polarized along the a axis, evincing the one-dimensional physics along the ET chain. The experiments were performed at room temperature.

Figure 3(c) reports the spectrally integrated time-resolved reflectivity changes $\Delta R/R$ in ET-F_2TCNQ for a

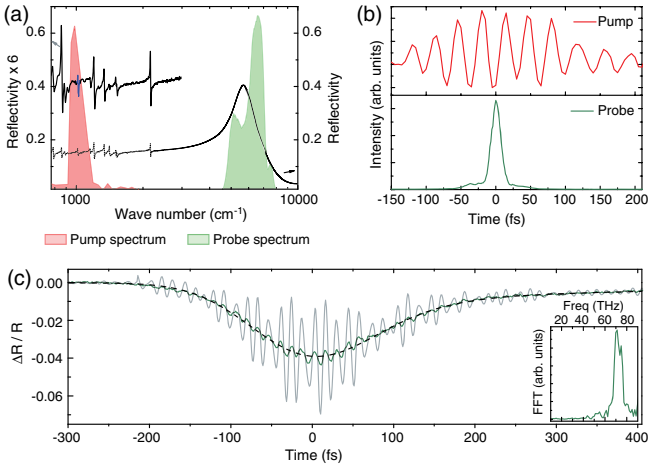

FIG. 3 (color online). (a) (red) Spectrum of the midinfrared excitation pulses centered at 1000 cm^{-1} (10 μm wavelength) resonant to the ET molecular vibration mode (blue). The sample reflectivity in direction perpendicular to the a axis is shown in gray. (green) The spectrum of the near-infrared probe beam covers the charge transfer band along the a axis. (b) (upper panel) Phase-locked electric field of the midinfrared pump pulse measured via electro-optic sampling; (lower panel) intensity profile of NIR probe pulse. (c) (green) Spectrally integrated time-dependent reflectivity changes in ET-F_2TCNQ at a pump fluence of 0.9 mJ/cm^2 at room temperature, together with a double exponential fit of the form $A\mathrm{erf}(t/t_d+1)\sum_{i=1,2}A_i e^{-t/\tau_i}$ in dashed black. The gray solid line shows the deconvolved reflectivity changes, and the inset shows a Fourier transformation of the measured oscillations peaking at 70 THz.

pump fluence of 0.9 mJ/cm^2 obtained by detecting the energy of the reflected probe pulses with a photodiode using the lock-in technique. The reflectivity was observed to reduce by 4% during the pump pulse, recovering in 45 fs along the trailing edge of the pump pulse and followed by a slower exponential decay of 500 fs. The fast decay is attributed to the direct relaxation of the driven vibrational mode. The slower response is attributed to lattice thermalization. Crucially, fast oscillations at approximately 70 THz were observed, with an amplitude of 0.7%. Note that these oscillations are convolved with the 10 fs duration of the probe pulse, longer than their 8 fs half-period, thus, reducing their amplitude. In the same figure, we also show the response after deconvolution, now exhibiting oscillations of about the same amplitude as the overall reduced reflectivity [gray trace in Fig. 3(c)].

The microscopic origin of these dynamics appears to follow qualitatively the response discussed above for quadratic coupling of the type $\hat{H}_{e\text{-vib}} = (C/2)B_2[1-\cos(2\Omega_{\mathrm{IR}}\tau)]\hat{n}_{j\uparrow}\hat{n}_{j\downarrow}$. For a 1D system, any change in filling will bring the system into a metallic state [24]. Since no metallic Drude response is observed in the terahertz regime [11], we can rule out a transient deviation from the average band filling as the origin of the experimentally observed oscillations. Further insight was possible by performing a spectrally resolved pump-probe measurement using a gated spectrometer for the detection of the probe. The time-dependent reflectivity spectrum is shown in Fig. 4(a), evidencing a reduction in the total reflectivity (from a peak value of 0.4 to 0.33), a red shift of the reflectivity peak (by ~70 cm^{-1}), and oscillations with the same 70 THz frequency detected in the spectrally integrated measurements of Fig. 3(c). The observed reflectivity change in Fig. 4(a) is consistent with the spectrally integrated data in Fig. 3(c) when integrating the spectral changes over the weighted probe spectral content. From this reflectivity spectrum, the optical conductivity was calculated at each time delay by a Kramers-Kronig (KK) consistent variational dielectric function fit [25]. The results are reported in Fig. 4(b), clearly showing oscillations of the conductivity spectrum.

We next analyze the measured response by fitting these transient conductivity spectra. As discussed in Refs. [26–28], the charge transfer band of ET-F_2TCNQ in equilibrium is described by two dominant contributions to the optical conductivity [see Fig. 4(c)]. The rather strong peak at lower frequency is related to holon-doublon (HD) pair excitations, that is, the transfer of charges between

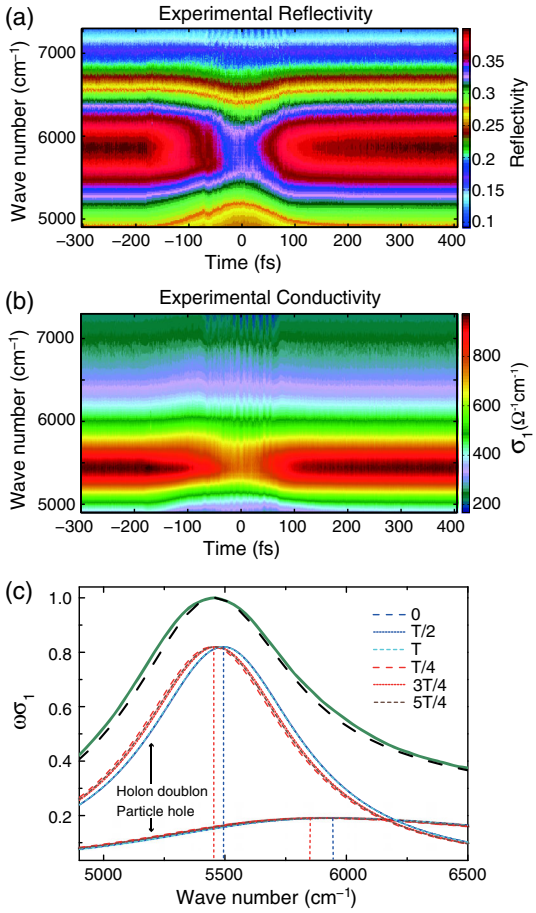

FIG. 4 (color online). (a) Frequency-resolved reflectivity as a function of pump-probe delay time. (b) Corresponding optical conductivity extracted from reflectivity using the KK variational dielectric fit function. (c) Normalized equilibrium optical conductivity (green) of ET-F_2TCNQ at room temperature with model fit (dashed black). Below are the fitted contributions from the HD and PH continuum, individually normalized at various times along the pump electric field cycle of time period T.

neighboring ET sites. As this holon-doublon exciton is bound by the intersite Coulomb correlation V, its energy is centered at $U - V - 4t^2/V$ [28]. A second weaker contribution to the conductivity spectrum results from the excitation of delocalized holon-doublon pairs not bound by the intersite Coulomb energy V [15], which form a particle-hole (PH) continuum described by a band of width $8t$ centered at U [27].

Figure 4(c) reports the fit results of the optical conductivity in which individually normalized contributions from bound HD pairs and PH continuum are displayed in intervals of ¼ of the time period of the pump electric field. We find that the peak positions of both HD and PH oscillate at 70 THz frequency, synchronized with the molecular mode. We extract U and V, fitting the optical conductivity along the lines described in Ref. [27], as a function of pump-probe delay time. Assuming that the hopping amplitude does not oscillate with the driven local vibrational motion [29], this procedure yields the effective correlation term U/t and V/t. Crucially, the overall reduction of U/t is superimposed by a response at frequency $2\Omega_{\mathrm{IR}}$, consistent with a quadratic coupling of U to the vibrational degree of freedom [see Fig. 5(a)]. V/t also shows a prominent reduction contributing to the transient changes [Fig. 5(c)] but does not show oscillatory behavior. Note that as for the spectrally integrated measurements, the spectral shifts [35 cm^{-1} (4 meV) and 93 cm^{-1} (12 meV) wavenumbers for HD and PH features, respectively] and the corresponding estimate of the U/t modulations are strongly underestimated because our probe beam is longer than the limit of 8 fs. No attempt to deconvolve this resolution factor was made for the U/t parameter, although the response is likely to be 1 order of magnitude larger than estimated here. Note also that the absolute changes induced by the pump in U and V are of comparable magnitude, 7 and 14 meV, respectively. Finally, we observe that the 70 THz oscillations are at slightly higher frequency than twice the excitation frequency (60 THz). This effect is likely related to the precision of our measurement. However, we cannot exclude that second-order effects may be taking place, beyond the considerations discussed in Eq. (2). No attempt was made to analyze these possible effects, which may involve, for example, a change in frequency of the vibrations by fourth-order coupling, potentially squeezing the vibration [30,31].

Additional theoretical analysis further substantiates the coherent modulation of the Hubbard U parameter. An effective model describing electronic excitations above the insulating ground state in the strong-coupling limit was used (see the Supplemental Material [32]), allowing for a numerical computation of the optical conductivity from the nonequilibrium two-time current-current correlation function $\chi_{JJ}(\tau,\tau') = \langle 0|\hat{\mathcal{U}}^\dagger(\tau+\tau')\hat{J}\hat{\mathcal{U}}(\tau+\tau')\hat{\mathcal{U}}^\dagger(\tau')\hat{J}\hat{\mathcal{U}}(\tau')|0\rangle$ [33–35]. In this expression, $\hat{\mathcal{U}}(\tau)$ is the time-evolution operator of the system up to time τ including time dependence caused by the driving, and $\hat{J}$ is the current operator. We assumed that U varies in time as a Gaussian pulse envelope superimposed with the $q^2_{\mathrm{IR}}(\tau)$ oscillation as $U(\tau) = U\{1 - A_U e^{-(\tau-\tau_P)^2/T_P^2}[1 - P_0 q^2_{\mathrm{IR}}(\tau)]\}$, where τ_P and T_P are the center and width of the pulse taken from the experiment, and A_U quantifies the overall reduction of U seen from the equilibrium fitting in Fig. 5(a). Only the parameter P_0 giving the amplitude of the oscillations around the envelope was fitted, giving a profile shown in Fig. 5(b). We assumed that V varies only with the envelope [Fig. 5(d)]. The computed $\chi_{JJ}(\tau,\tau')$ was then transformed into the simulated reflectivity and simulated conductivity shown in Figs. 5(e) and 5(f) and is seen to give an excellent reproduction of measured reflectivity and conductivity shown in Figs. 4(a) and 4(b). In order to rule out a modulation of the nearest-neighbor interaction, we repeated these calculations also under the assumption of an oscillatory V/t ratio. The calculated optical properties

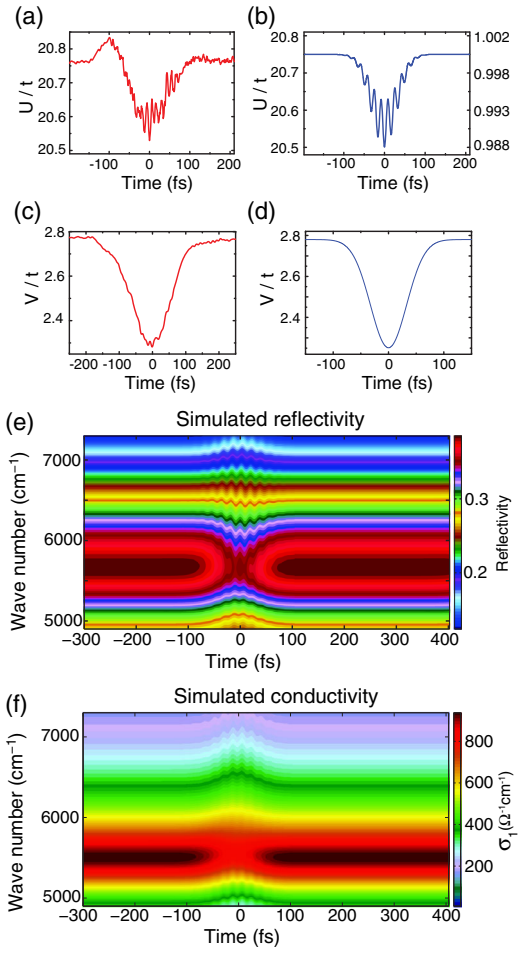

FIG. 5 (color online). (a),(c) Time dependence of effective Hubbard correlation term U/t and V/t, respectively, extracted from fits. (b) and (d) Assumed U/t and V/t variation, respectively, over time for numerical simulation, similar to one obtained experimentally. (e) Simulated reflectivity obtained via two-time current-current correlation function calculations of an effective strong-coupling model. (f) Corresponding simulated conductivity from the calculations.

(reported in Fig. 3 of the Supplemental Material [32]) differ significantly from the experimental observations, further supporting the claim that the on-site U modulation is the dominant effect behind the oscillatory behavior.

In summary, the time-dependent reflectivity of the molecular Mott insulator ET-F_2TCNQ shows a coherent modulation of the correlation gap following phase-stable vibrational excitation. The nonlinear characteristic of the coupling is evidenced by the response, which occurs at approximately twice the frequency of the driving pulse. Fitting of the time-dependent optical conductivity reveals that the on-site Hubbard U parameter is being directly modulated by the excitation of the local molecular vibration. This is in contrast to what was discussed to date for the excitation of collective phonon modes. Vibrational control may be combined with midinfrared pulse-shaping techniques [36], well established in the visible spectral range [37,38], and open up new avenues to coherently control interactions in a many-body system, a task to date only possible with cold-atom optical lattices via the Feshbach resonance [35].

We acknowledge financial support the European Research Council under the European Union's Seventh Framework Programme (FP7/2007-2013)/ERC Grant Agreement No. 319286 Q-MAC.

*rashmi.singla@mpsd.mpg.de
†s.kaiser@fkf.mpg.de
‡andrea.cavalleri@mpsd.mpg.de

[1] M. Först, C. Manzoni, S. Kaiser, Y. Tomioka, Y. Tokura, R. Merlin, and A. Cavalleri, Nonlinear phononics as an ultrafast route to lattice control, Nat. Phys. **7**, 854 (2011).

[2] M. Rini, R. Tobey, N. Dean, J. Itatani, Y. Tomioka, Y. Tokura, R. W. Schoenlein, and A. Cavalleri, Control of the electronic phase of a manganite by mode-selective vibrational excitation, Nature (London) **449**, 72 (2007).

[3] M. Först, R. I. Tobey, S. Wall, H. Bromberger, V. Khanna, A. L. Cavalieri, Y.-D. Chuang, W. S. Lee, R. Moore, W. F. Schlotter, J. J. Turner, O. Krupin, M. Trigo, H. Zheng, J. F. Mitchell, S. S. Dhesi, J. P. Hill, and A. Cavalleri, Driving magnetic order in a manganite by ultrafast lattice excitation, Phys. Rev. B **84**, 241104(R) (2011).

[4] D. Fausti, R. Tobey, N. Dean, S. Kaiser, A. Dienst, M. Hoffmann, S. Pyon, T. Takayama, H. Takagi, and A. Cavalleri, Light-induced superconductivity in a stripe-ordered cuprate, Science **331**, 189 (2011).

[5] W. Hu, S. Kaiser, D. Nicoletti, C. R. Hunt, I. Gierz, M. C. Hoffmann, M. Le Tacon, T. Loew, B. Keimer, and A. Cavalleri, Optically enhanced coherent transport in $YBa_2Cu_3O_{6.5}$ by ultrafast redistribution of interlayer coupling, Nat. Mater. **13**, 705 (2014).

[6] S. Kaiser, C. R. Hunt, D. Nicoletti, W. Hu, I. Gierz, H. Y. Liu, M. Le Tacon, T. Loew, D. Haug, B. Keimer, and A. Cavalleri, Optically induced coherent transport far above T_c in underdoped $YBa_2Cu_3O_{6+\delta}$, Phys. Rev. B **89**, 184516 (2014).

[7] A. Subedi, A. Cavalleri, and A. Georges, Theory of nonlinear phononics for coherent light control of solids, Phys. Rev. B **89**, 220301(R) (2014).

[8] R. Mankowsky, A. Subedi, M. Foerst, S. O. Mariager, M. Chollet, H. Lemke, J. Robinson, J. Glownia, M. Minitti, A. Frano, M. Fechner, N. A. Spaldin, T. Loew, B. Keimer, A. Georges, and A. Cavalleri, Nonlinear lattice dynamics as a basis for enhanced superconductivity in $YBa_2Cu_3O_{6.5}$, Nature (London) **516**, 71 (2014).

[9] P. Guionneau, C. J. Kepert, G. Bravic, D. Chasseau, M. R. Truter, M. Kurmoo, and P. Day, Determining the charge distribution in BEDT-TTF salts, Synth. Met. **86**, 1973 (1997).

[10] K. Itoh, H. Itoh, M. Naka, S. Saito, I. Hosako, N. Yoneyama, S. Ishihara, T. Sasaki, and S. Iwai, Collective excitation of an electric dipole on a molecular dimer in an organic dimer-Mott insulator, Phys. Rev. Lett. **110**, 106401 (2013).

[11] S. Kaiser, S. R. Clark, D. Nicoletti, G. Cotugno, R. I. Tobey, N. Dean, S. Lupi, H. Okamoto, T. Hasegawa, D. Jaksch, and A. Cavalleri, Optical properties of a vibrationally modulated solid state Mott insulator, Sci. Rep. **4**, 3823 (2014).

[12] T. Yamamoto, M. Uruichi, K. Yamamoto, K. Yakushi, A. Kawamoto, and H. Taniguchi, Examination of the charge-sensitive vibrational modes in Bis(ethylenedithio) tetrathiafulvalene, J. Phys. Chem. B **109**, 15226 (2005).

[13] A. Girlando, Charge sensitive vibrations and electron-molecular vibration coupling in Bis(ethylenedithio)-tetrathiafulvalene (BEDT-TTF), J. Phys. Chem. C **115**, 19371 (2011).

[14] H. Okamoto, H. Matsuzaki, T. Wakabayashi, Y. Takahashi, and T. Hasegawa, Photoinduced Metallic State Mediated by Spin-Charge Separation in a One-Dimensional Organic Mott Insulator, Phys. Rev. Lett. **98**, 037401 (2007).

[15] S. Wall, D. Brida, S. R. Clark, H. P. Ehrke, D. Jaksch, A. Ardavan, S. Bonora, H. Uemura, Y. Takahashi, T. Hasegawa, H. Okamoto, G. Cerullo, and A. Cavalleri, Quantum interference between charge excitation paths in a solid-state Mott insulator, Nat. Phys. **7**, 114 (2011).

[16] T. Hasegawa, S. Kagoshima, T. Mochida, S. Sugiura, and Y. Iwasa, Electronic states and anti-ferromagnetic order in mixed-stack charge-transfer compound (BEDT-TTF) (F_2TCNQ), Solid State Commun. **103**, 489 (1997).

[17] H. Uemura, H. Matsuzaki, Y. Takahashi, T. Hasegawa, and H. Okamoto, Ultrafast charge dynamics in one-dimensional organic Mott insulators, J. Phys. Soc. Jpn. **77**, 113714 (2008).

[18] This assumption is justified since the strongly coupled local molecular vibrations are well separated (~400–1600 cm^{-1}) from the weakly coupled lattice phonons of the comparably heavy molecular sites (below 200 cm^{-1}).

[19] T. Holstein, Studies of polaron motion: Part1. The molecular-crystal model, Ann. Phys. (N.Y.) **8**, 325 (1959).

[20] J. E. Hirsch, Dynamic Hubbard Model, Phys. Rev. Lett. **87**, 206402 (2001).

[21] R. Huber, A. Brodschelm, F. Tauser, and A. Leitenstorfer, Generation and field-resolved detection of femtosecond electromagnetic pulses tunable up to 41 THz, Appl. Phys. Lett. **76**, 3191 (2000).

[22] C. Manzoni, M. Först, H. Ehrke, and A. Cavalleri, Single-shot detection and direct control of carrier phase drift of midinfrared pulses, Opt. Lett. **35**, 757 (2010).

[23] D. Brida, G. Cirmi, C. Manzoni, S. Bonora, P. Villoresi, S. De Silvestri, and G. Cerullo, Sub-two-cycle light pulses

at 1.6 μm from an optical parametric amplifier, Opt. Lett. **33**, 741 (2008).

[24] T. Giamarchi, Mott transition in one dimension, Physica (Amsterdam) **230–232B**, 975 (1997).

[25] A. B. Kuzmenko, Kramers–Kronig constrained variational analysis of optical spectra, Rev. Sci. Instrum. **76**, 083108 (2005).

[26] E. Jeckelmann, Optical excitations in a one-dimensional Mott insulator, Phys. Rev. B **67**, 075106 (2003).

[27] M. Mitrano, G. Cotugno, S. R. Clark, R. Singla, S. Kaiser, J. Stähler, R. Beyer, M. Dressel, L. Baldassarre, D. Nicoletti, A. Perucchi, T. Hasegawa, H. Okamoto, D. Jaksch, and A. Cavalleri, Pressure-Dependent Relaxation in the Photoexcited Mott Insulator ET $-$ F_2TCNQ: Influence of Hopping and Correlations on Quasiparticle Recombination Rates, Phys. Rev. Lett. **112**, 117801 (2014).

[28] F. H. L. Essler, F. Gebhard, and E. Jeckelmann, Excitons in one-dimensional Mott insulators, Phys. Rev. B **64**, 125119 (2001).

[29] Note that the bandwidth $t = 40$ meV corresponds to a hopping time scale of 10 THz and, therefore, cannot follow a fast oscillatory modulation at 70 THz.

[30] G. A. Garrett, A. G. Rojo, A. K. Sood, J. F. Whitaker, and R. Merlin, Vacuum squeezing of solids: Macroscopic quantum states driven by light pulses, Science **275**, 1638 (1997).

[31] S. L. Johnson, P. Beaud, E. Vorobeva, C. J. Milne, E. D. Murray, S. Fahy, and G. Ingold, Directly Observing Squeezed Phonon States with Femtosecond X-Ray Diffraction, Phys. Rev. Lett. **102**, 175503 (2009).

[32] See the Supplemental Material at http://link.aps.org/supplemental/10.1103/PhysRevLett.115.187401 for detailed information on the fits to the optical conductivity data, and the simulations using the two-time correlation function.

[33] F. Gebhard, K. Born, M. Scheidler, P. Thomas, and S. W. Koch, Exact results for the optical absorption of strongly correlated electrons in a half-filled Peierls-distorted chain, Philos. Mag. B **75**, 13 (1997).

[34] F. Gebhard, K. Born, M. Scheidler, P. Thomas, and S. W. Koch, Optical absorption of strongly correlated half-filled Mott-Hubbard chains, Philos. Mag. B **75**, 47 (1997).

[35] I. Bloch, J. Dalibard, and W. Zwerger, Many-body physics with ultracold gases, Rev. Mod. Phys. **80**, 885 (2008).

[36] A. Cartella, S. Bonora, M. Först, G. Cerullo, A. Cavalleri, and C. Manzoni, Pulse shaping in the mid-infrared by a deformable mirror, Opt. Lett. **39**, 1485 (2014).

[37] C. J. Bardeen, V. V. Yakovlev, K. R. Wilson, S. D. Carpenter, P. M. Weber, and W. S. Warren, Feedback quantum control of molecular electronic population transfer, Chem. Phys. Lett. **280**, 151 (1997).

[38] J. C. Vaughan, T. Hornung, T. Feurer, and K. A. Nelson, Diffraction-based femtosecond pulse shaping with a two-dimensional spatial light modulator, Opt. Lett. **30**, 323 (2005).